Development 138, 1433-1444 (2011) doi:10.1242/dev.058016

Conditional ablation of *Pten* in osteoprogenitors stimulates FGF signaling

Anyonya R. Guntur[1], Martina I. Reinhold[2], Joe Cuellar, Jr[2] and Michael C. Naski[1,2,*]

SUMMARY

Phosphatase and tensin homolog deleted on chromosome ten (PTEN) is a direct antagonist of phosphatidylinositol 3 kinase. *Pten* is a well recognized tumor suppressor and is one of the most commonly mutated genes in human malignancies. More recent studies of development and stem cell behavior have shown that PTEN regulates the growth and differentiation of progenitor cells. Significantly, PTEN is found in osteoprogenitor cells that give rise to bone-forming osteoblasts; however, the role of PTEN in bone development is incompletely understood. To define how PTEN functions in osteoprogenitors during bone development, we conditionally deleted *Pten* in mice using the cre-deleter strain *Dermo1*cre, which targets undifferentiated mesenchyme destined to form bone. Deletion of *Pten* in osteoprogenitor cells led to increased numbers of osteoblasts and expanded bone matrix. Significantly, osteoblast development and synthesis of osteoid in the nascent bone collar was uncoupled from the usual tight linkage to chondrocyte differentiation in the epiphyseal growth plate. The expansion of osteoblasts and osteoprogenitors was found to be due to augmented FGF signaling as evidenced by (1) increased expression of FGF18, a potent osteoblast mitogen, and (2) decreased expression of SPRY2, a repressor of FGF signaling. The differentiation of osteoblasts was autonomous from the growth plate chondrocytes and was correlated with an increase in the protein levels of GLI2, a transcription factor that is a major mediator of hedgehog signaling. We provide evidence that increased GLI2 activity is also a consequence of increased FGF signaling through downstream events requiring mitogen-activated protein kinases. To test whether FGF signaling is required for the effects of *Pten* deletion, we deleted one allele of fibroblast growth factor receptor 2 (FGFR2). Significantly, deletion of FGFR2 caused a partial rescue of the *Pten*-null phenotype. This study identifies activated FGF signaling as the major mediator of *Pten* deletion in osteoprogenitors.

KEY WORDS: Endochondral ossification, *Pten*, Perichondrium, FGF18, *Dermo1*cre, Osteoprogenitors, Mouse

INTRODUCTION

Endochondral ossification is the process by which long bones in vertebrates develop. In mice, during this highly coordinated process mesenchymal cell condensations form at around 10.5 days post coitum (dpc) and differentiate into chondrocytes, thereby forming the template of the future bones. Thereafter, the chondrocytes undergo a series of highly coordinated processes leading to the formation of the growth plate. The future long bone at this stage is surrounded by a sheath of cells called the perichondrium (Kronenberg, 2003; Karsenty, 1999). The perichondrium is adjacent to and surrounds the epiphyseal growth plate. It contains osteoprogenitors required for appositional growth of the long bone (Colnot et al., 2004). Osteoprogenitors residing in the perichondrium supply the osteoblasts that migrate with blood vessels invading the hypertrophic chondrocytes, thereby establishing the primary ossification center with trabecular bone. The skeletal precursor cells in the perichondrium also supply osteoblasts that produce cortical bone (Colnot et al., 2004). Growth factors such as fibroblast growth factor (FGF) activate signaling pathways transduced by tyrosine kinase receptors. Data show that FGF receptors (FGFRs) play a key role in coordinating events during endochondral ossification; for example, activating mutations in FGFR1, FGFR2 and FGFR3 have been linked to various skeletal abnormalities that affect normal endochondral ossification (Muenke et al., 1994; Reardon et al., 1994; Rousseau et al., 1994). FGF ligands that are required for normal bone development include FGF 1, FGF2, FGF7, FGF8, FGF9, FGF17 and FGF18. These ligands effect bone development via binding to the cognate FGF receptors, which are normally expressed in bone, leading to activation of cellular signaling processes mainly through the Ras/MAP Kinase (mitogen-activated protein kinase), PKC (protein kinase C) and PI3K (phosphatidylinositol 3 kinase) cascades. (Ornitz, 2005; Miraoui and Marie, 2010).

Recent studies have shown that the PI3K signaling pathway has an important role in regulating bone development. PTEN is a lipid phosphatase that negatively regulates the PI3K signaling pathway. PTEN expression has been shown in chondrocytes and osteoblasts but the role it plays in bone formation signaling events has not been completely elucidated. Several recent studies (Ford-Hutchinson et al., 2007; Hsieh et al., 2009) reported the use of collagen2a1 cre to delete *Pten* in the cartilage of developing mice and saw defects in growth plate organization along with an increase in chondrocyte differentiation and increased bone formation resulting in skeletal overgrowth. Similar experiments carried out by Yang et al. (Yang et al., 2008) showed that the growth plate defects in collagen2a1 cre *Pten* cko mice resulted from increased endoplasmic reticulum stress in *Pten*-null resting chondrocytes. Other investigators (Liu et al., 2007) used an osteocalcin cre to delete *Pten* in mature osteoblasts. These data showed increased bone mass that accumulated throughout the animal's life span. Also, deletion of *Pten* in cultured calvarial osteoblasts led to accelerated differentiation with a decrease in cell death.

[1]Department of Biochemistry, University of Texas Health Science Center at San Antonio, 7703 Floyd Curl Drive, San Antonio, TX 78229, USA. [2]Department of Pathology, University of Texas Health Science Center at San Antonio, 7703 Floyd Curl Drive, San Antonio, TX 78229, USA.

*Author for correspondence (mikenaski@yahoo.com)

Accepted 6 January 2011

To define the role of PTEN in osteoprogenitors, we deleted *Pten* in mesenchymal condensations of nascent bones using the *Dermo1*cre deleter strain. *Dermo1* (*Twist2* – Mouse Genome Informatics) expression is turned on at 9.5 dpc in mice, thereby allowing us to study the role of *Pten* in osteoprogenitors (Li et al., 1995; Yu et al., 2003). We observed robust knockout of PTEN in the perichondrium using the *Dermo1*cre deleter strain. *Pten* deletion led to increased bone formation. Significantly, osteoblast differentiation was geographically altered in the *Pten* conditional knockouts. In addition to bone formation in the usual distribution, we found osteoblasts in regions of the perichondrium away from the hypertrophic chondrocytes. This suggested a differentiation pathway for a subset of osteoblast progenitors that is autonomous of growth plate control. We discovered that deletion of *Pten* stimulates FGF signaling. Activation of FGF signaling occurs via a bipartite pathway. First, the expression of the ligand FGF18 is increased and second, the FGF antagonist SPRY2 is decreased. This increase in FGF signaling stimulates osteoprogenitor cell expansion. We queried whether the increase in FGF signaling contributes to the autonomous osteoblast differentiation. We discovered an increase in the hedgehog-dependent transcription factor GLI2 in *Pten*-deleted perichondrium. Additional results support a model whereby the increase in GLI2 is driven by signaling downstream of FGFRs. Finally, the *Pten*-null phenotype was partially rescued by removing one allele of the major perichondrial FGFR, FGFR2. This study identifies for the first time that *Pten* deletion leads to an increase in FGF signaling, which can stimulate both perichondrial cell proliferation and osteoblast differentiation.

MATERIALS AND METHODS

Real-time quantitative PCR

Total RNA was extracted from cultured primary osteoblasts or immortalized preosteoblasts following a protocol described previously (Kapadia et al., 2005). Primer sequences used were (5′-3′): 18s_Fwd, CATGTGGTGTTGAGGAAAGCA; 18s_Rev, GTCGTGGGTTCTGCATGATG; Pten_Fwd, GACCAGAGACAAAAAGGGAGTCA; Pten_Rev, GTGCCACGGGTCTGTAATCC; BGLAP2_e1-3_A_Fwd, ACCTTATTGCCCTCCTGCTT; BGLAP2_e1-3_A_Rev, CTTGGTGCACACCTAGCAGA; BGLAP2_e3-4_A_Fwd, TTTGTAGGCGGTCTTCAAGA; BGLAP2_e3-4_A_Rev, AAGCAGGAGGGCAATAAGGT; SPRY2_Fwd, TATTTGCACATCGCTGGAAG; SPRY2_Rev, CTCCATCAGGTCTTGGCAGT; FGF18_A/B_Fwd, ACTGCTGTGCTTCCAGGTTC; FGF18_A_Rev, CCCAGGACTTGCATGTGCTT; FGF18_B_Rev, CCCAGGACTTGAATGTGCTT; SPP1_e1-3_A_Fwd, TGAGATTGGCAGTGATTTGC; SPP1_e1-3_A_Rev, TGGCTATAGGATCTGGGTGC; Osterix_Fwd, CCACTGGCTCCTCGGTTCT; Osterix_Rev, GTCCCGCAGAGGGCTAGAG. The data was analyzed using the method described by Livak and Schmittgen (Livak and Schmittgen, 2001). All data represent expression relative to 18s.

BrdU and TUNEL labeling for proliferation and apoptosis studies

Bromodeoxyuridine (BrdU) labeling and immunohistochemistry was carried out following protocols described previously (Naski et al., 1998; Kapadia et al., 2005). Apoptotic cells in the long bones were identified by using TUNEL labeling of nicked DNA. Labeling was carried out by utilizing biotin-16-dUTP (Boehringer Mannheim) and terminal deoxynucleotidyl transferase (Gibco) to label nicked DNA. A DAB substrate kit (Vector Laboratories) was utilized to develop and visualize apoptotic cells.

Primary calvarial osteoblasts isolation and culture

One-day-old *Pten* flox/flox pups were sacrificed and the calvaria were dissected and collected in 1× Hank's buffered saline solution with 10% penicillin and streptomycin. The collected whole calvaria were gently scraped to remove any adhered tissue and digested in a buffer containing 0.5% trypsin, 0.2% collagenase. The calvaria were digested for 15 minutes in a 6-well plate in 3 ml of buffer shaken continuously in an incubator maintained at 37°C, humidified 5% CO_2. The first two digests were discarded and the remaining six digests were collected and cultured in 10% FBS-alpha-MEM. The cells that were collected after counting were plated in 1 ml 10% FBS-alpha-MEM and cultured as required to examine osteoblast differentiation. This protocol was modified from a rat calvaria isolation protocol (Yeh et al., 1996).

Metatarsal rudiment dissection and culture

Metatarsal rudiments were dissected from 15.5 dpc embryos obtained when *Pten* flox/flox females were mated with *Pten* flox/wt and *Dermo1*cre heterozygous males. The dissected metatarsal rudiments were cultured as described previously (Kapadia et al., 2005).

In situ hybridization

Radiolabeled riboprobes were synthesized by in vitro transcription reaction and used to label paraffin embedded tissue as described previously (Naski et al., 1996).

Immunohistochemistry and immunofluorescence

Immunohistochemistry was performed on paraffin-embedded tissue using a tyramide amplification kit (Perkin Elmer) following the manufacturer's instructions. For immunofluorescence on cells plated on cover slips for AdGFP-AdCRE and 40 μg/ml BrdU (Sigma) treatments we followed the protocols described previously (Kapadia et al., 2005; Geng et al., 2009).

Mice genotyping and processing

Mice tail snips were processed overnight in a solution containing proteinase K (40 μg/ml), 1 M Tris (pH 8.0), 5 M sodium chloride, 0.5 M EDTA (pH 8.0) and 10% SDS, and digested at 55°C. 1 μl of the extracted and resuspended DNA was utilized in a PCR reaction. *Pten* flox/flox mice, *Fgfr2* flox/flox and *Dermo1*cre mice were described previously (Suzuki et al., 2001; Yu et al., 2003). The animals were maintained in accordance with protocols approved by the animal care committee at the University of Texas Health Science Center at San Antonio.

Western blotting

Protein lysates were prepared and run on SDS-PAGE gels as reported previously (Reinhold and Naski, 2007).

Plasmids and antibodies

To create shRNAi plasmids, purified oligonucleotides were cloned into the pSiren Shuttle expression vector. For generating stable transformants, a neomycin resistance gene from pcDNA3.1 was cloned into the pSiren Shuttle vector using compatible *Xho*I and *Bgl*II sites. Sequences used were: shRNAi *Pten* top strand, GATCCAGTAGAGTTCTTCTTCCACAAATTCAAGAGATTTGTGGAACTCTACTTTTTTTACGCGTG; shRNAi *Pten* bottom strand, AATTCACGCGTAAAAAAAGTAGAGTTCTTCCACAAATCTCTTGAATTTGTGGAAGAACTCTACTG; shRNAi control top strand, GATCCAATTCTCCGAACGTGTAAATTCAAGAGATTTACACGTTCGGAGAATTTTTTTTACGCGTG; shRNAi control bottom strand, AATTCACGCGTAAAAAAAATTCTCCGAACGTGTAAATCTCTTGAATTTACACGTTCGGAGAATTG. The plasmid for generating the in situ hybridization probe for osterix (*Sp7* – Mouse Genome Informatics) was made as follows: 1285 bp of the mouse osterix coding sequence was cloned into an pSP72 vector, *Bam*HI was used to digest the plasmid and T7 RNA polymerase was utilized to create the antisense riboprobe. *Col1a1*, osteopontin (*Spp1* – Mouse Genome Informatics), *Fgf18*, *Pthr1* (*Pth1r* – Mouse Genome Informatics) and patched (*Ptch1* – Mouse Genome Informatics) in situ hybridization probes have been reported elsewhere (Yu et al., 2003; Reinhold and Naski, 2007; Naski et al., 1998). Other plasmids used were: pECE_FoxO3aAAA [kindly provided by Dr Burgering (Brunet et al., 1999)], pGL3_8XGli_luc (Cooper et al., 2003), pFC_CaMEK1, pcDNAS45A_bcat, pGL3FGF18, 3.4kbLuc, pCMV_Runx2 and pCS_FGFR3K650E. (Reinhold and Naski, 2007; Naski et al., 1996).

Antibodies used were: anti-sprouty2 (Sigma, S1819), goat anti-FGF18 (Santa Cruz Biotechnology, sc16830), anti-Pten (Cell Signaling, 9559), anti-pAktSer473 (Cell Signaling, immunohistochemistry specific 3787), anti-pAktSer473 (Cell Signaling, 9271), anti-Akt (Cell Signaling, 9272), anti-pErk (p44/42MAPK Thr202/Tyr204 Cell Signaling, 4370) or anti-pErk (Santa Cruz, sc7383), anti-Erk (Zymed Laboratories, mouse anti-MAP Kinase ERK1+ERK2), anti-Gli2 (Rockland 600-401-695) and anti-actin (mouse monoclonal, Chemicon International) (Kapadia et al., 2005; Reinhold et al., 2006).

Transfections, nucleofections and luciferase assays

Transient transfections were carried out using a calcium phosphate precipitation method as reported in Reinhold et al. (Reinhold et al., 2006). Nucleofection was used to transfect shRNAi expressing Pten and scrambled control into C3H10T1/2 cells to look at the effect of knockdown of Pten on FGF18 (Reinhold and Naski, 2007).

Histology and skeletal staining

Newborn pups were dissected in 1× PBS and fixed overnight in 4% paraformaldehyde (PFA), followed by 14% EDTA solution for decalcification for 2 weeks. Standard methods were followed for embedding, sectioning 5-μm tissue sections and Hematoxylin and Eosin (H&E) staining (Naski et al., 1996). Skeletal preparations of newborn pups was carried out following the protocol by Mcleod (Mcleod, 1980). Von Kossa staining was carried out following a protocol described by Zhao et al. (Zhao et al., 2002).

microCT

The hind limbs and fore limbs of newborn mice were dissected and fixed in 4% PFA. The undecalcified limbs were wrapped in foam and put into 15-ml tubes. The samples were packed tightly so that there were no air bubbles. For 27 μm scans a GE eXplore machine was utilized. The data that was obtained was analyzed using MicroView (open source software from GE). Using this software the femurs were first separated from the total scans and the volumetric bone mineral density (BMD) of whole femurs from the *Pten* conditional knockouts were compared with the wild-type controls from postnatal day one (Vasquez et al., 2008).

Statistical analysis

All the experiments were repeated at least three times. *P* value was calculated using Student's *t*-test and the null hypothesis was rejected for *P* values <0.05.

RESULTS

Effective knockout of *Pten* using *Dermo1*cre

PTEN, a lipid phosphatase and tumor suppressor protein (Li et al., 1997; Myers et al., 1998), is expressed in both chondrocytes and osteoblasts (Fig. 1A). To study the role of *Pten* during bone development, we deleted *Pten* in mesenchymal cell condensations prior to cell fate decisions using the *Dermo1*cre deleter strain. *Pten* was efficiently deleted in osteoblasts and perichondrial osteoprogenitor cells as observed by the loss of indirect immunofluorescence staining for PTEN (Fig. 1A) in mice inheriting the *Dermo1*cre allele. PTEN was also deleted in chondrocytes (Fig. 1A). PTEN negatively regulates phosphatidylinositol-3 kinase (PI3K) signaling (Stambolic et al., 1998) and, therefore, ablation of *Pten* should upregulate PI3K signaling, including phosphorylation of the PI3K dependent kinase AKT (AKT1 – Mouse Genome Informatics). As expected, Fig. 1A shows increased phosphorylation of AKT at serine 473 following PTEN loss. Additionally, osteoblasts isolated from clavaria of newborn *Pten* knockout pups showed a decrease in *Pten* at the mRNA level (Fig. 1B).

Skeletal abnormalities observed when *Pten* is deleted using *Dermo1*cre

We examined the gross skeletal morphology of the *Pten* conditional knockouts and the wild-type controls by staining with Alcian blue and Alizarin red. Fig. 2A shows that the femurs, as well as other long bones of the conditional knockouts were shorter (Fig. 2G) and broader than those of the wild-type controls. To examine the architectural and cellular basis of the skeletal changes, we prepared histological sections stained with H&E. Light microscopic

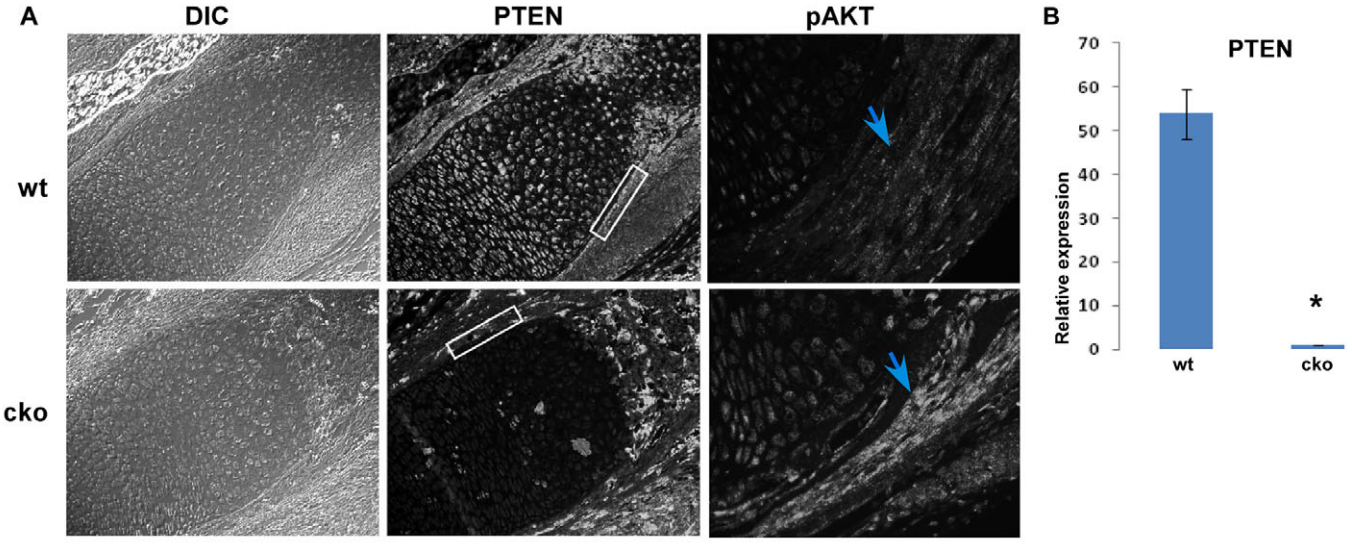

Fig. 1. Knockout of *Pten* using *Dermo1*cre. (**A**) Immunofluorescence images showing the loss of PTEN in both chondrocytes and osteoblasts (white boxes). The top panel shows wild-type (wt) tibial sections and the bottom panel shows those of the conditional knockout (cko) mouse. The right-hand panel shows the concomitant increase in pAKTSer473 (blue arrows) following PTEN deletion using *Dermo1*cre. Differential interference contrast (DIC) images are shown on the left. (**B**) Relative mRNA levels from wt and *Dermo1*cre *Pten* cko calvarial osteoblasts isolated from newborn pups (n=3, *P<0.05). Error bars indicate s.d.

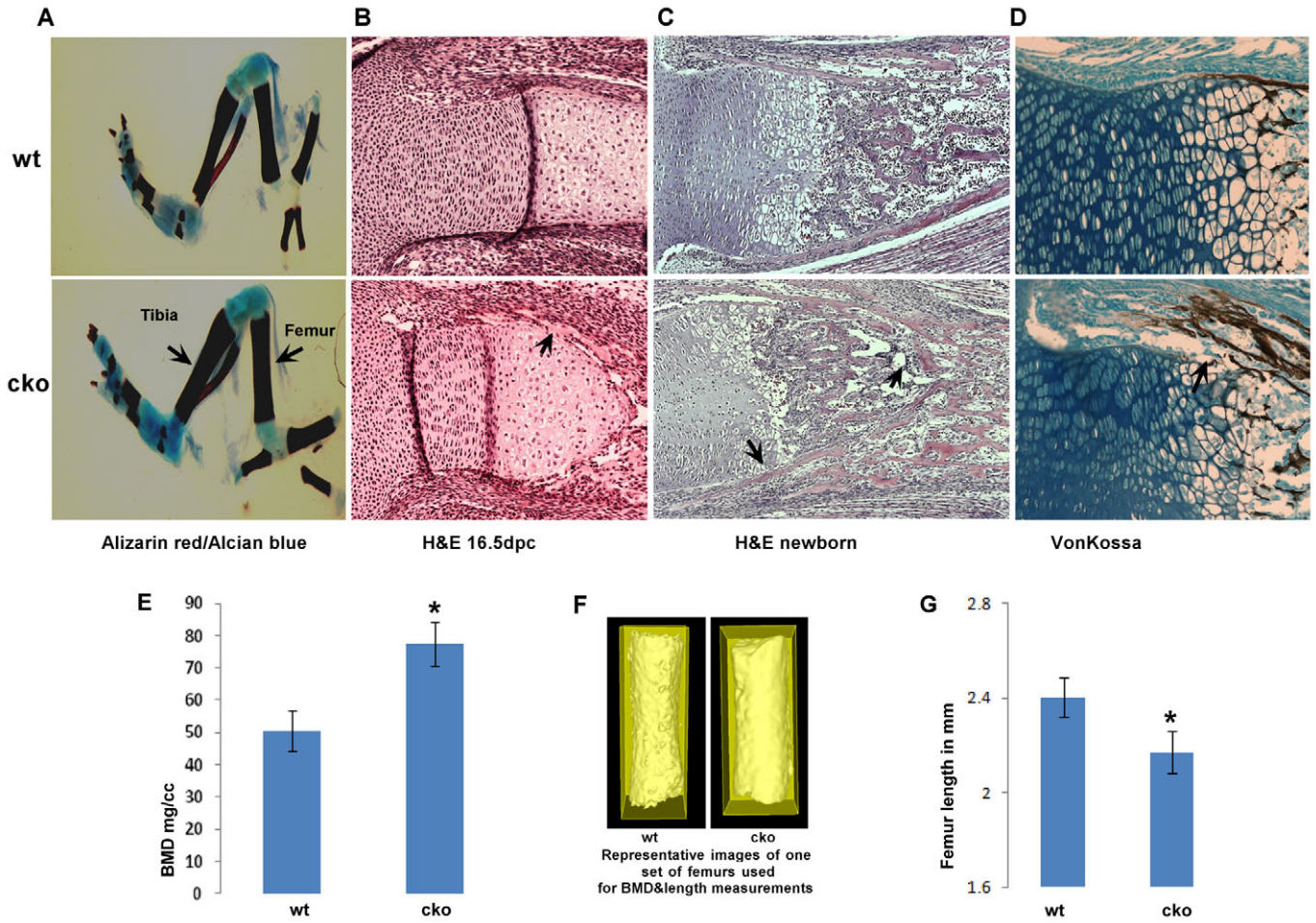

Fig. 2. Gross skeletal morphology, histology and microCT analysis. (**A**) Wild-type (wt) and conditional knockout (cko) Alizarin red- and Alcian blue-stained mouse hindlimbs showing the thicker tibia and femur (black arrows) in the *Dermo1*cre cko compared with those in the wt control. (**B**,**C**) Hematoxylin and Eosin (H&E) staining on 16.5 days post coitum (dpc) and one-day-old tibial sections showing increased osteoid formation in the perichondrial region (black arrows) in the cko compared with the wt control. (**D**) Von Kossa staining on newborn undecalcified tibial sections showing increased mineralization in the perichondrium of the *Pten* knockout (black arrow). (**E**) Bone mineral density (BMD) determined by 27 μm microCT imaging of femurs from 1-day-old wt and cko showing a significant increase in BMD (n=3, *P<0.005). Error bars indicate s.d. (**F**) Representative 27 μm microCT femur reconstruction data used to calculate the BMD and lengths of the femurs shown as bar graphs in E and G. (**G**) Length of femurs from 1-day-old wt and cko showing a significant decrease in length (n=3, *P<0.05). Error bars indicate s.d.

examination of the *Pten* conditional knockout and wild-type tibia at 16.5 dpc and one day postnatal (Fig. 2B,C) showed an increase in perichondral and trabecular bone in the conditional knockouts (ckos). Interestingly, the ckos displayed multiple layers of perichondrial osteoid bone. A single layer of osteoid was deposited directly on top of the hypertrophic chondrocytes in the wild-type mice; however, the ckos displayed layers of osteoid at increasing distance from the hypertrophic chondrocytes. To assess the mineralization of the bone, we performed Von Kossa staining on undecalcified tibial sections and, consistent with the increased osteoid, we saw increased bone mineralization in the ckos (Fig. 2D). These findings were further substantiated by microCT analysis of femurs, which showed increased bone mineral density (BMD) at 1 day old (Fig. 2E,F).

Loss of *Pten* increases perichondrial cell proliferation

We found an increase in bone matrix and BMD in the ckos (Fig. 2C,E). Inspection of the histological sections showed a parallel increase in osteoblast numbers. To determine whether deletion of *Pten* leads to an increase in cell proliferation we performed BrdU labeling studies. Significantly, the ckos demonstrated increased BrdU labeling in the perichondrium compared with the wild-type control (Fig. 3A,B). An alternative explanation for the increased osteoblast number is a reduced rate of cell death. We, therefore, tested for apoptosis using TUNEL labeling and saw only scattered cells that were positive for TUNEL in the perichondrium of the humerus sections (see Fig. S1A in the supplementary material). There was no significant difference in the number of apoptotic cells (see Fig. S1B in the supplementary material).

Pten knockout increased osteoblast differentiation

We have shown augmented bone matrix in the *Pten* ckos and have morphologically coupled this matrix to increased numbers of osteoblasts. We next wished to determine whether these cells expressed normal markers of osteoblast differentiation. Assays of gene expression by in situ hybridization showed normal levels of markers of osteoblast differentiation in the *Pten* ckos (Fig. 4A-D) but significantly increased levels in the perichondral region. To determine whether expression is upregulated developmentally and

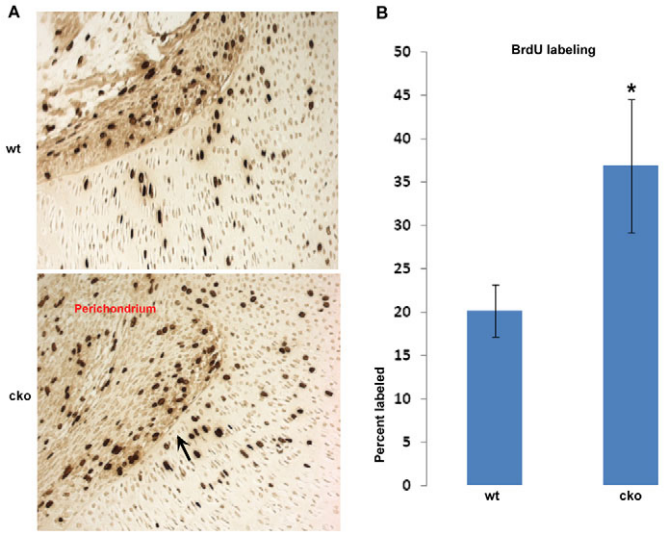

Fig. 3. Cell proliferation studies using BrdU labeling. (**A**) Immunohistochemistry for BrdU labeled cells (dark brown) using a BrdU antibody on paraffin-embedded tissue sections. The arrow indicates the border of the perichondrium region. (**B**) The number of BrdU-labeled and total cells in the perichondrium (the region adjacent to the growth plate) of *Pten* conditional knockout (cko) and wild-type (wt) tibiae were counted and plotted as the percentage of BrdU labeled cells. A significant increase in cell proliferation was observed in the perichondrium of the cko relative to wt (n=3, *P<0.005). Error bars indicate s.d.

in other skeletal elements, we looked at *Col1a1* at 16.5 dpc tibial and 18.5 dpc humerus sections and observed a similar increase in expression in the *Pten* conditional knockouts compared with the wild-type controls (data not shown). Significantly, the expression of the gene encoding the PTH/PTHrP receptor (*Pthr1*; *Pth1r* – Mouse Genome Informatics) was unchanged in the chondrocytes (Fig. 4E).

Increased FGF signaling in the absence of *Pten*

We found increased cell proliferation in the *Pten* ckos. Given that fibroblast growth factors are essential regulators of skeletal growth, we hypothesized that FGF signaling might contribute to the increase in cell proliferation. Because *Fgf18* is expressed in the perichondrium and is an important osteoblast mitogen, we examined *Fgf18* expression in the perichondrium of osteoblast markers using in situ hybridization. Significantly, we found increased *Fgf18* expression in the *Pten* ckos compared with the wild-type control (Fig. 5A). To confirm this, we examined FGF18 protein using immunohistochemistry and, similarly, we observed increased levels in the periosteum of *Pten* ckos (Fig. 5B). Because we observed increased FGF18 expression we also queried whether there is altered antagonism of FGF. The sprouty proteins inhibit FGF signaling by decoupling intracellular connections of the FGF receptor with the Ras-Raf signaling axis (Hacohen et al., 1998; Gross et al., 2001). Recently, data show that *Spry2* expression is inhibited by PI3K activity (Paik et al., 2007). We examined SPRY2 protein in the *Pten* ckos by immunohistochemistry. Significantly, deletion of *Pten* led to reduced SPRY2 in the perichondrium compared with the wild-type control (Fig. 5C).

To evaluate more closely the pathways leading to increased *Fgf18* expression, we investigated whether the FOXO transcription factors regulate *Fgf18* expression. The FOXO transcription factors

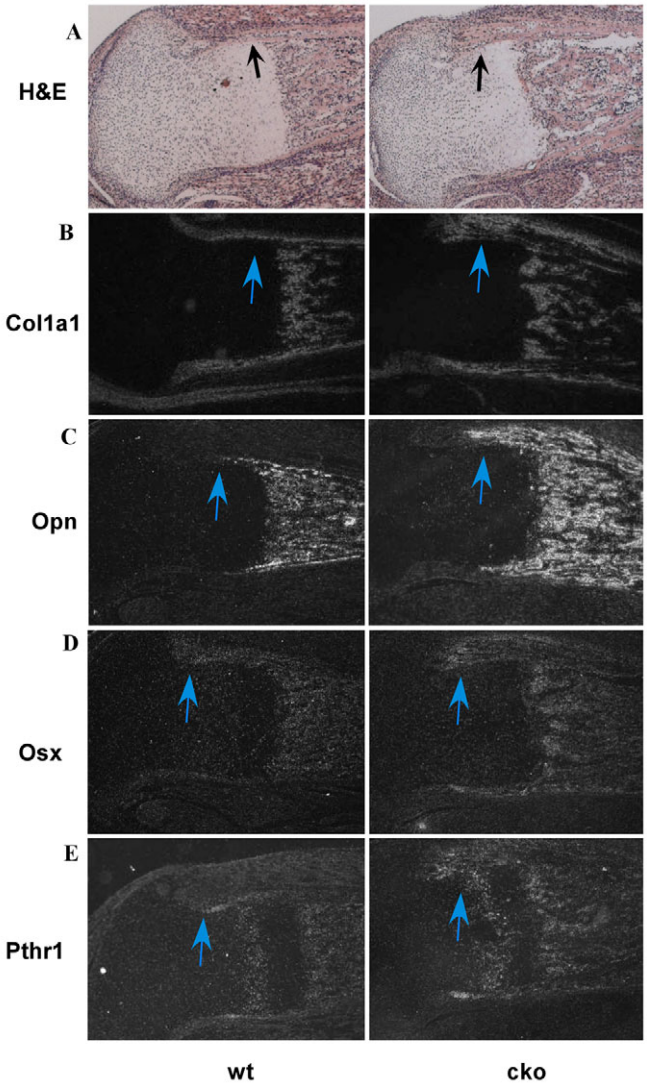

Fig. 4. Expression of osteoblast markers in wild-type (wt) and *Pten* conditional knockout (cko) mice. (**A**) Hematoxylin and Eosin (H&E) staining on newborn tibial sections. Black arrows indicate the perichondrium region. (**B**) In situ hybridization on tibial sections using a *Col1a1*-radiolabeled probe showed an increase in transcript level in the cko relative to wt. (**C-E**) Transcript levels of the osteoblast differentiation markers osteopontin (Opn; C) and osterix (Osx; D) were substantially increased in the cko compared with the wt in both the perichondrium (blue arrows indicate the perichondrium) and the primary ossification region, whereas there was no difference in the expression pattern of *Pthr1* (E).

are phosphorylated in response to PI3K activity and this phosphorylation leads to export from the nucleus and repression of FOXO transcription (Brunet et al., 1999). We first asked whether *Fgf18* expression can be regulated by FOXOs. Overexpression of FOXO3A (constitutively active; FOXO3 – Mouse Genome Informatics) in the preosteoblast cell line C3H10T1/2 led a twofold suppression of *Fgf18* mRNA levels (Fig. 5D). shRNAi-mediated knockdown of PTEN (Fig. 5E′) in C3H10T1/2 led to a twofold increase in *Fgf18* (Fig. 5E), supporting the view that FGF18 expression is positively regulated by PI3K signaling, which acts to release the inhibition of FGF18 by FOXO transcription factors. This was investigated more directly using an FGF18 luciferase

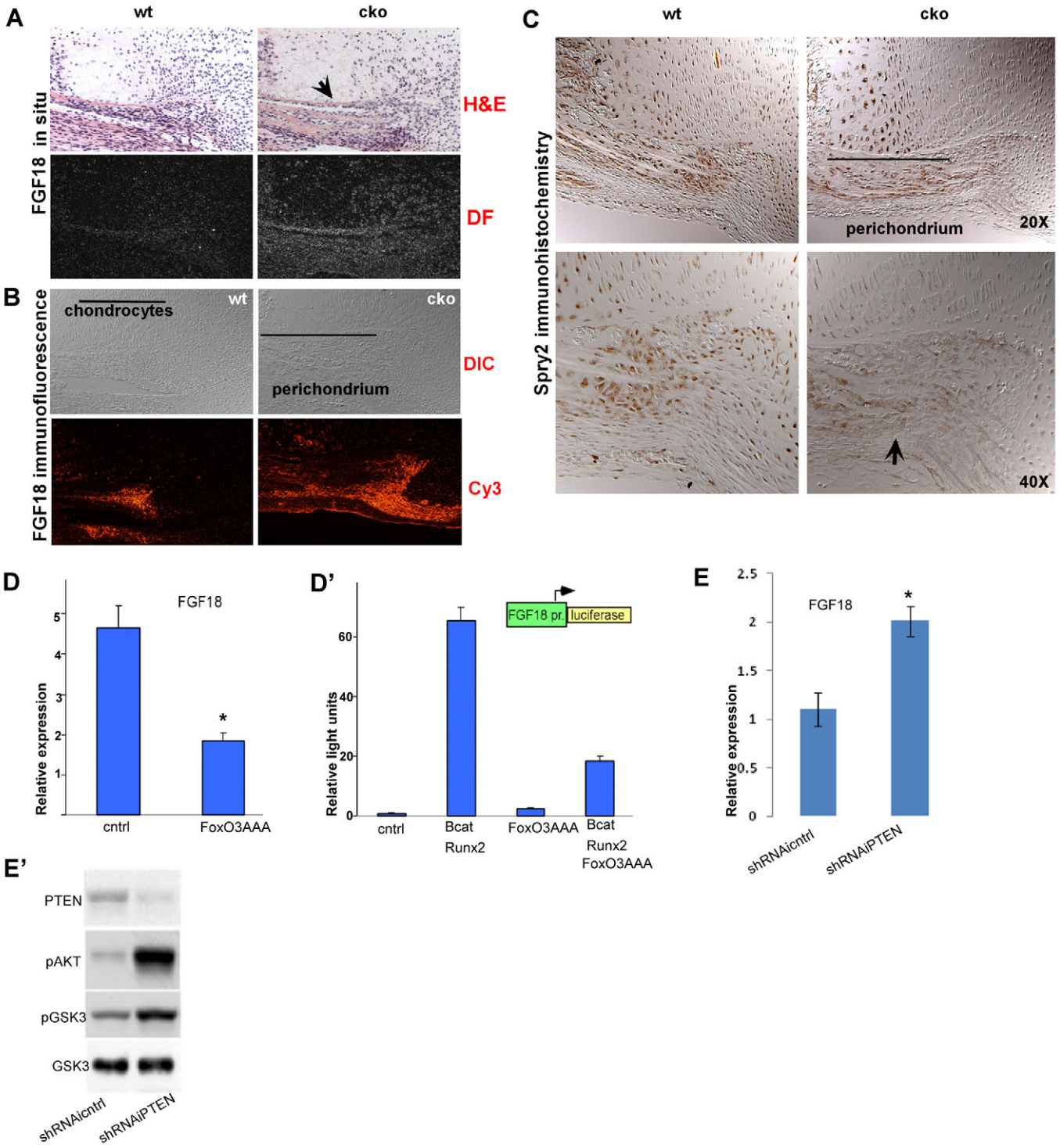

Fig. 5. Effect of *Pten* deletion on FGF signaling. (**A**) In situ hybridization on *Pten*-deleted newborn tibial sections shows increased *Fgf18* transcript levels in the perichondrium of *Pten* conditional knockout (cko) mice compared with wild type (wt), as can be observed in the dark field (DF) images. The perichondrial region is indicated with a black arrow in the H&E panel. (**B**) Immunofluorescence of FGF18 reveals a substantial increase in expression in the periosteum of the *Pten* cko compared with the wt. Black lines indicate growth plate in wt and the perichondrium in the cko. (**C**) Immunohistochemistry for SPRY2 expression shows decreased protein levels in the perichondrium (black arrow) of cko mice compared with wt. Black line indicates the perichondrium. (**D**) Overexpression of FOXO3A (FoxO3AAA) in C3H10T1/2 cells resulted in suppression of *Fgf18* expression (n=3, *P<0.05). (**D'**) Foxo3A also inhibited the FGF18 promoter luciferase expression, which is activated by RUNX2 (Runx2) and beta-catenin (Bcat). Luciferase activity was normalized to β-galactosidase activity as shown by a co-transfected plasmid (repeated at least three times). (**E**) shRNAi-mediated knockdown of *Pten* (shRNAiPTEN) in C3H10T1/2 cells showed an increase in FGF18 transcript levels when compared with scrambled control (shRNAicntrl) (n=3, *P<0.05). (**E'**) Western blot showing that shRNAi can specifically knockdown PTEN protein expression and activate AKT in MC3T3E1 cells. All error bars indicate s.d. DIC, differential interference contrast.

reporter plasmid. In previous work we showed that the *Fgf18* gene expression is directly induced through a bipartite binding element that is recognized by RUNX2 and the WNT-dependent transcription factors TCF4 and LEF1 (Reinhold and Naski, 2007). In Fig. 5D′ we show that a constitutively active form of FOXO3A inhibited the activation of the FGF18 luciferase reporter, whereas in the absence of RUNX2 and beta-catenin, FOXO3A had relatively little effect on FGF18 expression. To study further the effect of activated PI3K activity on *Spry2*, we knocked out *Pten* in *Pten* flox/flox primary calvarial osteoblasts using AdenoCRE and studied *Spry2* expression in response to basic fibroblast growth factor (bFGF). In control AdenoGFP cells, *Spry2* was induced as expected; however, the induction of *Spry2* was blunted in the knockdown cells (see Fig. S2 in the supplementary material). This corroborates the findings of decreased SPRY2 protein in the cko mice (Fig. 5C).

Osteoblast differentiation in ckos is independent of endochondral ossification

The development of osteoblasts in the perichondrium is tightly coupled to the differentiation of chondrocytes in the growth plate. During normal growth and development osteoblasts form adjacent to and synthesize bone matrix directly on hypertrophic chondrocytes. Because osteoblasts in ckos developed at sites uncoupled from the chondrocyte hypertrophy, we hypothesized that *Pten* knockout osteoblasts develop autonomously from chondrocytes. To test this, we used the metatarsal rudiment culture system wherein osteoblast development is stringently coupled to endochondral chondrocyte differentiation. We anticipated that if osteoblast hyperplasia and development was driven by chondrocyte hypertrophy, then the metatarsals from ckos should show similar expansion of osteoblasts and bone. Metatarsal bone rudiments were isolated from 15.5 dpc embryos of wild type and *Pten* cko and cultured in serum-free conditions. Fig. 6A shows deletion of PTEN using immunofluorescence. The metatarsals at 15.5 dpc lacked hypertrophic chondrocytes as well as osteoblasts. Therefore, development of perichondrial osteoblasts is strongly driven by chondrocyte differentiation. Importantly, there was no significant difference in osteoblast development in the *Pten* ckos compared with the wild-type littermates (Fig. 6B,C), supporting the view that expanded osteoblast development in *Pten* ckos is not secondary to an alteration in chondrocytes differentiation in the ckos and that expanded osteoblast differentiation is uncoupled from chondrocyte differentiation in the growth plate.

Effect of *Pten* deletion on GLI2 and osteoblast differentiation

Hedgehog signaling is essential for osteoblast differentiation and the effect of hedgehog is largely determined by the GLI transcription factors. Because we observed an increase in osteoblast differentiation, we questioned whether this might be due to increased GLI2. Significantly, immunofluorescence staining showed an increase in GLI2 levels in ckos compared with the wild-type control (Fig. 7A). The increase in GLI2 prompted us to look at targets of GLI2 transcription, namely, patched. In situ hybridization for the patched transcript revealed increased signal in the *Pten* ckos relative to littermate controls (Fig. 7B). As our data showed that FGF signaling is augmented in the ckos, we investigated whether an activated FGF receptor (K650E) can stimulate Gli transcriptional activity. We transfected C3H10T1/2 preosteoblast cells with a *Gli2* reporter plasmid, and found that the activity of GLI2 was increased when co-transfected with a plasmid expressing activated FGF receptor (Fig. 7C). Similarly, dose-dependent activation of GLI2 was observed when co-transfected with an activated form of MEK (Fig. 7C′), suggesting that activation of GLI2 by FGF signaling is through a MAP kinase cascade. We further substantiate a role for increased MAP kinase activity in *Pten* knockout cells. Calvarial osteoblasts were isolated from mice with homozygous floxed alleles for *Pten*, then cultured in vitro and infected with either AdenoCRE or AdenoGFP to produce *Pten* knockout or control osteoblasts, respectively. MAP kinase activity was then measured by western blotting and immunofluorescence staining for phospho-extracellular signal-related kinase (pERK). Significantly, western blotting showed that *Pten*-null osteoblasts have increased pERK and, in addition, knockout osteoblasts had increased nuclear pERK (Fig. 7D,E).

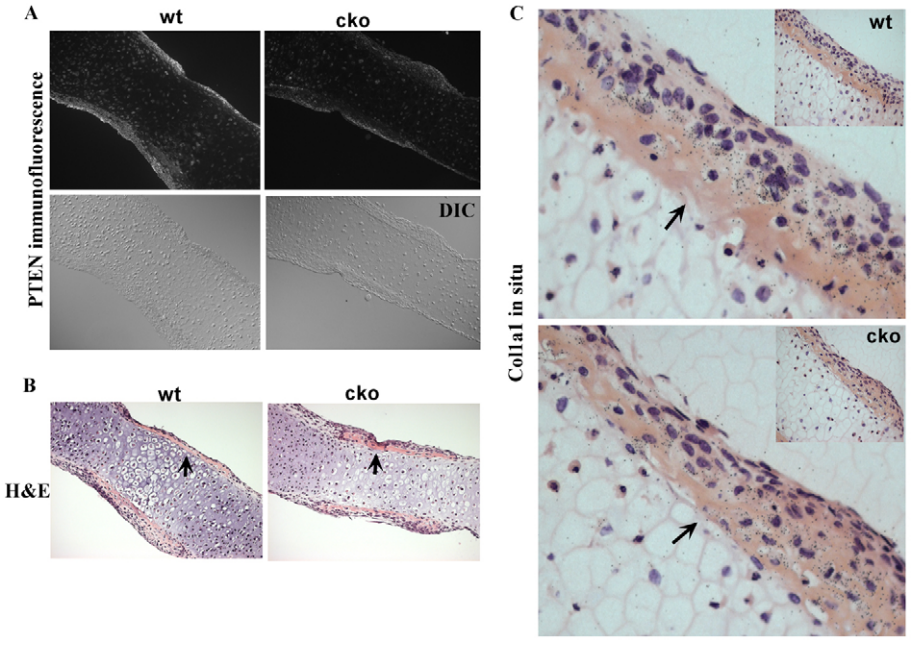

Fig. 6. Metatarsal rudiments isolated from the hindlimbs of wild-type (wt) and *Pten* conditional knockout (cko) mice at 15.5 dpc and cultured in vitro to study the cell-autonomous effect of the *Pten* knockout. (**A**) Immunofluorescence for PTEN on metatarsal rudiments showing loss of PTEN protein in the cko. (**B**) Hematoxylin and Eosin (H&E)-stained metatarsal rudiments showing no difference in osteoblast differentiation in the absence of PTEN (black arrows indicate osteoid). (**C**) *Col1a1* in situ hybridization showing no change in the expression of *Col1a1* mRNA. Black arrows indicate the perichondrium. Insets are low power images of the rudiments. DIC, differential interference contrast.

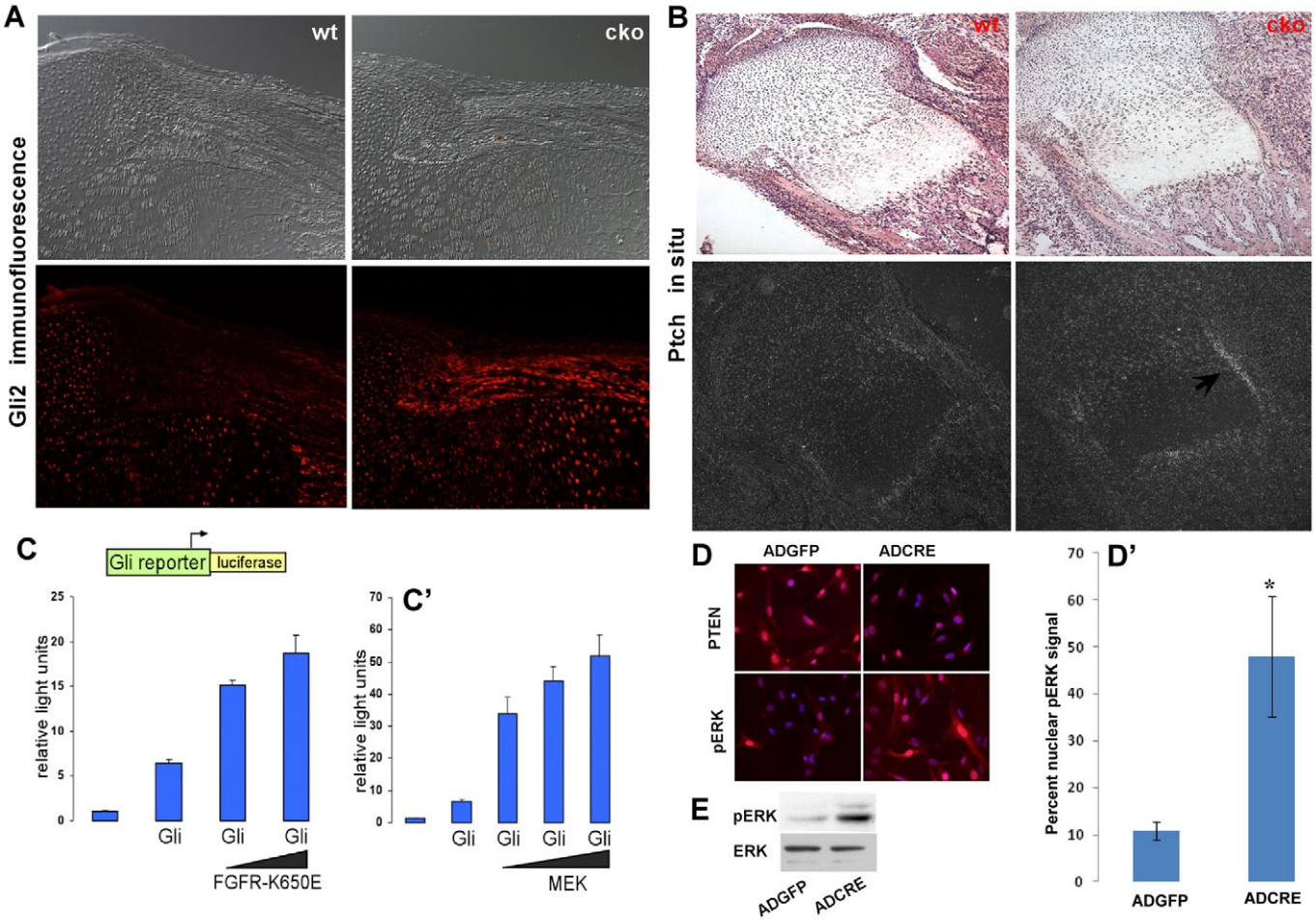

Fig. 7. Effect of *Pten* deletion on hedgehog signaling. (**A**) Immunofluorescence of GLI2 showed an increase in the expression of osteoblasts that line the perichondrium in the *Pten* conditional knockout (cko) compared with wild type (wt). (**B**) In situ hybridization for patched (*Ptch1*), a transcriptional target for GLI2, showed an increase (black arrow) in *Ptch1* expression in the cko compared with the wt control. (**C**,**C'**) Using a *Gli2* luciferase reporter plasmid transfected into C3H10T1/2 cells we observed that there is an activation of *Gli2* transcription when an active form of FGFR (FGFR-K650E) is co-transfected with GLI2. We also observed an increase in *Gli2* luciferase activity when we used an activated MEK kinase plasmid (repeated at least three times). Black wedges indicate increasing concentrations of FGFR-K650E or MEK co-transfected with Gli2. Luciferase activity was normalized to β-galactosidase activity. (**D**) Using *Pten* flox/flox calvarial osteoblasts, we used AdenoGFP (ADGFP) as control and AdenoCRE (ADCRE) to delete PTEN as can be observed in the indirect immunofluorescence images in the top panels. When PTEN is deleted we observe an increase in pERK nuclear localization. (**D'**) The number of cells with a nuclear pERK signal was determined revealing a significant increase in pERK (n=3, $^*P$<0.005). Images are overlays of DAPI (blue) and rhodamine (red) staining. (**E**) Western blot data for pERK and total ERK from protein lysates of *Pten* flox/flox calvarial osteoblasts treated with AdenoCRE and AdenoGFP. All error bars indicate s.d.

Rescue of the *Pten* phenotype by deletion of *Fgfr2*

Through several lines of evidence we have shown that FGF signaling is increased in the ckos and that this leads to increased MAP kinase activity. We hypothesized that the increased osteoprogenitor cell proliferation and osteoblast differentiation are a consequence of increased signaling through FGF receptors. We then reasoned that removal of an FGF receptor should reverse or ameliorate the phenotype. Therefore, we crossed a null allele for fibroblast growth factor receptor 2 (FGFR2) into the mating scheme. Deletion of one *Fgfr2* gene has no deleterious effects and is silent phenotypically (Yu et al., 2003). We choose *Fgfr2* because it is the major FGFR expressed in bone. Fig. 8A shows a partial rescue of the phenotype with a decrease of the perichondral bone phenotype. As seen previously, histological sections showed an increased perichondrial bone present in the *Pten* cko; however, there was a dramatic decrease in the amount of perichondrial bone in the *Pten* cko lacking an allele of *Fgfr2* (Fig. 8A). In situ hybridization for the molecular marker *Col1a1* (Fig. 8A′) showed an increase in expression in the *Pten* cko and this was attenuated in the cko lacking an allele for FGFR2. The rescue of the phenotype was probed further by examining GLI2 protein in the perichondrium. Significantly, protein levels of GLI2 were diminished in the perichondrium of the *Pten* cko lacking an allele of *Fgfr2* (Fig. 8B).

Primary osteoblast culture

Our data of metatarsal rudiment cultures suggest cell autonomous differentiation of the *Pten*-null osteoprogenitor cells. To address this more directly we prepared *Pten*-null calvarial osteoblasts and analyzed the differentiation of these cells in culture. *Pten* flox/flox calvarial osteoblasts were isolated from newborn pups and recombinant adenoviruses transducing cre-recombinase or GFP were used to make knockout and control cells, respectively. Western blotting showed efficient deletion of PTEN and a corresponding increase in pAKT. Using real-time PCR we assayed for indicators of

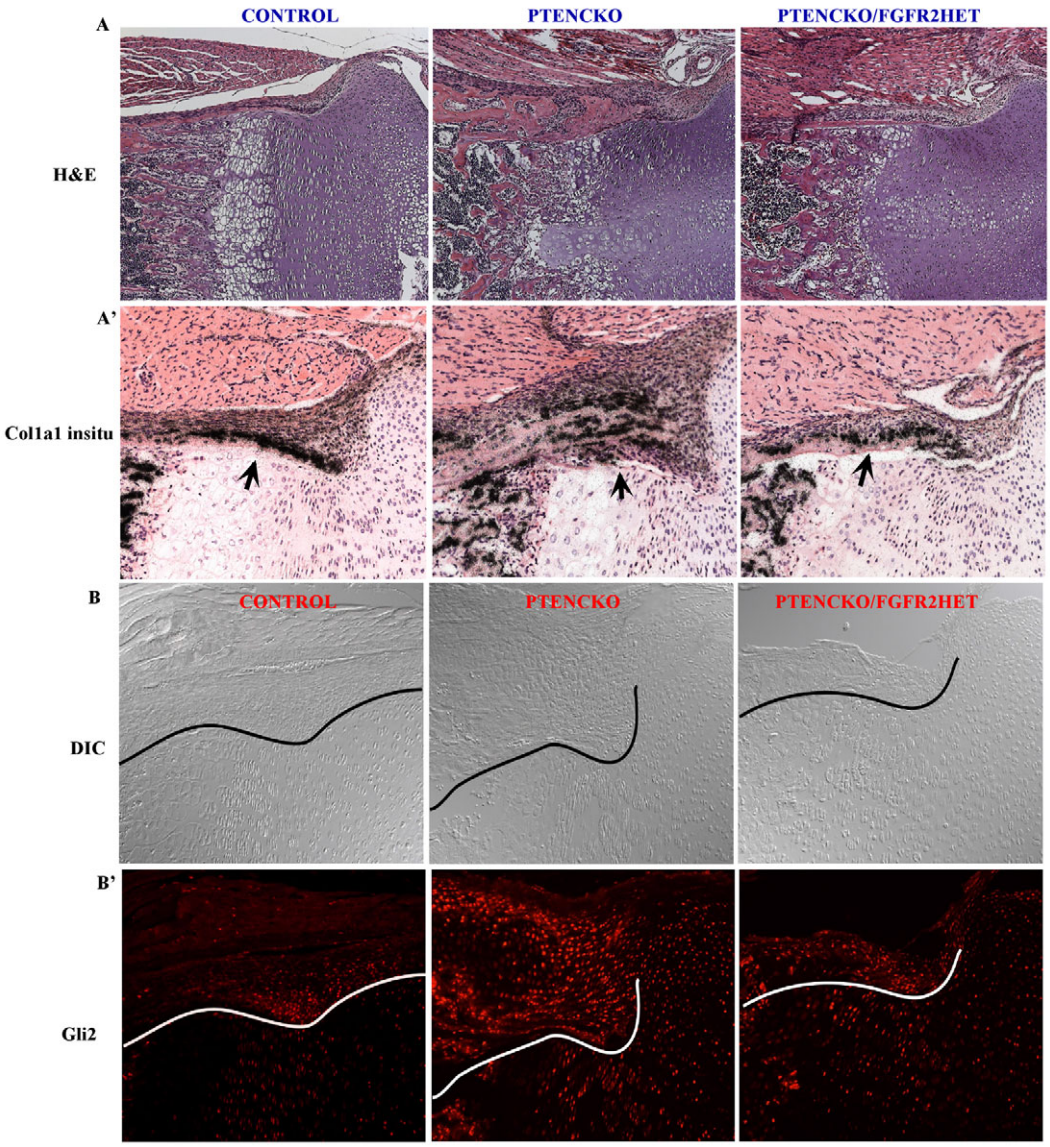

Fig. 8. Rescue of the *Pten* conditional knockout (cko) mouse phenotype by deletion of one allele of *Fgfr2*. (**A**,**A'**) Hematoxylin and Eosin (H&E) staining of the phenotype observed in the perichondrium, along with *Col1a1* in situ hybridization showing the increased perichondrium (black arrows) phenotype in the absence of *Pten* (PTENCKO). This phenotype is partially rescued with the deletion of *Pten* in the background of global loss of one allele of *Fgfr2* (PTENCKO/FGFR2HET). (**B**,**B'**) Immunohistochemistry for GLI2 protein levels in the perichondrium of tibial sections showed a similar increase in GLI2 protein levels in the absence of *Pten* but the GLI2 levels are comparable to the wild-type levels in the *Fgfr2* het *Pten* cko (PTENCKO/FGFR2HET) perichondrium. The conditional knockouts were generated using the *Dermo1*cre mouse strain. DIC, differential interference contrast.

osteoblast differentiation. Significantly, the relative expression of osteocalcin, osteopontin and osterix genes was increased in the PTEN cko cells. In addition, FGF18 expression was increased and *Spry2* was decreased, supporting our data indicating that FGF signaling is increased. We also characterized the proliferation of calvarial cells lacking PTEN and found increased proliferation (BrdU labeling) in PTEN-null cells. (Fig. 9A-C). Von Kossa staining on calvarial cells lacking PTEN showed increased bone nodule formation compared with control cells (Fig. 9D).

DISCUSSION

PTEN is a lipid phosphatase that directly antagonizes PI3K (Stambolic et al., 1998). Genetic disruption of *Pten* therefore leads to unchecked PI3K signaling (Sun et al., 1999). Recent data demonstrate that PTEN is essential for normal growth and development of skeletal cells. Conditional deletion of *Pten* in chondrocytes using collagen2a1 cre deleter mice leads to activation of stress response pathways and disruption of chondrocyte differentiation with development of a chondrodysplasia along with increased lipoma formation (Ford-Hutchinson et al., 2007; Yang et al., 2008; Hsieh et al., 2009). *Pten* deletion in end-stage, mature osteoblasts using osteocalcin cre leads to an increase in bone mass with a parallel increase in cell proliferation (Liu et al., 2007). Other studies knocking-out the downstream effectors AKT1 and AKT2 showed a delay in ossification (Peng et al., 2003). Deletion of *Pten* in osteoblasts certainly results in increased PI3K signaling by activating downstream kinase AKTs, but how this affects skeletal cell proliferation or skeletal cell differentiation is not clear. This

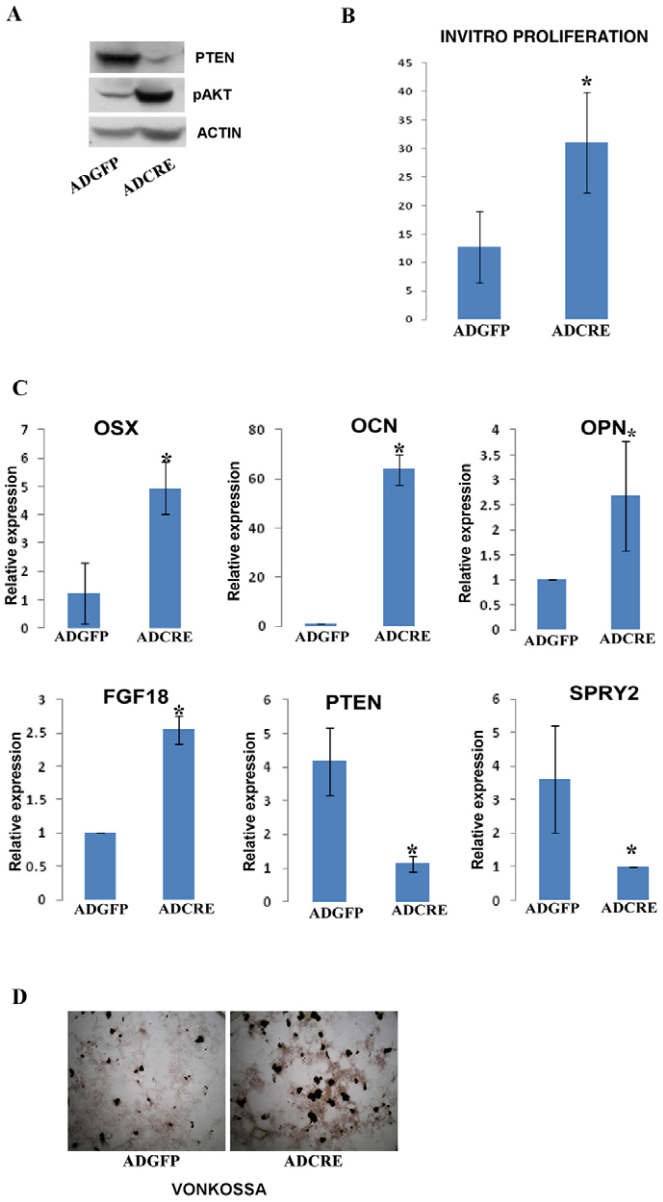

Fig. 9. Calvarial osteoblast isolation and culture. (**A**) *Pten* flox/flox primary calvarial osteoblasts were infected with AdenoGFP (ADGFP) and AdenoCRE (ADCRE) viruses to look at knockout efficiency of *Pten* and downstream activation of pAKTSer473. Actin was used as a loading control. (**B**) In vitro proliferation assay on *Pten* flox/flox primary calvarial osteoblasts that were infected with AdenoGFP and AdenoCRE viruses. Osteoblasts were plated at a low density and then labeled with BrdU after allowing sufficient time for proliferation. Indirect immunofluorescence was carried out on the cells to detect nuclear BrdU; cells showing positive stain in the nucleus were counted in a field of view (n=4, *P<0.05). (**C**) Relative mRNA levels for the osteoblast markers were obtained from samples that were cultured in differentiation media. After deletion of *Pten* for 13 days (by ADCRE), osterix (OSX; n=4, *P<0.0005), osteocalcin (OCN; n=3, *P<0.005), osteopontin (OPN; n=3, *P<0.005) and FGF18 (n=3, *P<0.05) showed an increase in expression in the CRE treated samples. *Pten* (PTEN; n=3, *P<0.05) and *Spry2* (SPRY2; n=3, *P<0.05) expression was decreased in the absence of *Pten*. (**D**) Von Kossa staining for bone nodule formation was was carried out on primary clavarial osteoblasts that were treated with the AdenoGFP and AdenoCRE viruses and cultured for 21 days in differentiation media containing β-glycerophosphate and ascorbic acid. All error bars indicate s.d.

study looks at these crucial issues by deleting *Pten* in osteoprogenitor cells and identifies increased FGF signaling as the major mediator of increased bone formation in the absence of PTEN.

Gross morphology, histology and osteoblasts marker expression

To investigate the pathways downstream of PTEN that influence bone, we created conditional null mice using the *Dermo1*cre deleter mice and mice having floxed *Pten* alleles. The majority of cko mice died in the perinatal period. Although the cause of death is not entirely clear it is probably due to respiratory failure, which might be secondary to inelasticity of the ribs. The limbs from ckos exhibited increased bone mass and asynchronous development of perichondrial osteoblasts. Our evidence indicates that this is due to increased proliferation of perichondrial cells and subsequent cell autonomous differentiation of these perichondrial cells into osteoblasts. Normally, the differentiation of the osteoblasts in the perichondrium is strictly coupled to the maturation of chondrocytes in the growth plate. Hypertrophic chondrocytes in the growth plate produce indian hedgehog and this in turn signals to perichondrial cells to induces osteoblast differentiation (Vortkamp et al., 1996). Significantly, we have found that osteoblast differentiation in the perichondrium of *Pten* ckos is uncoupled from the growth plate. Interestingly, the differentiation of *Pten*-null perichondrial cells still appears to require hedgehog-dependent signals; however, our data suggest that differentiation might not require a hedgehog ligand. Activation of hedgehog signaling might occur downstream of receptor-ligand dependent events. Activation of MAP kinase cascades through FGFR signaling might stabilize the transcription factor GLI2, which in turn might regulate differentiation of the cells into osteoblasts.

Increased FGF signaling in the absence of *Pten*

Pten cko mice demonstrated increased cell proliferation in the perichondrium (Fig. 3). Because of this, we hypothesized that there is increased growth factor signaling in *Pten* cko mice. To investigate this possibility we examined FGF18. We chose to study FGF18 because (1) it is expressed in the perichondrium at the site of increased proliferation and (2) it is a principle regulator of bone cell growth (Liu et al., 2002; Ohbayashi et al., 2002). Significantly, we showed that the expression of FGF18 is increased in the perichondium of ckos, consistent with the view that expansion of the perichondrial osteoprogenitors is FGF dependent. The increase in FGF18 expression appears to be, in part, a reflection of increased transcription of FGF18. We provide evidence that the forkhead transcription factor FOXO3 represses FGF18 expression. The repressor activity is therefore relieved when FOXO3 is exported from the nucleus in the face of increased PI3K signaling. Other evidence also points to increased FGF signaling. Specifically, we showed a relative decrease in the levels of the FGF signaling antagonist SPRY2. This implies that FGF signaling is amplified by two pathways: increased ligand and decreased post-receptor antagonism. These results suggest that a reduction of FGF receptor signaling could have a major effect on the consequences of deleting *Pten* in osteoprogenitor cells. To test this, we dampened FGF signaling by introducing a null allele for FGF receptor 2 (*Fgfr2*) into the mating scheme. *Fgfr2* is the major FGFR expressed in the perichondrium (Yu et al., 2003). Significantly, removal of a single allele of *Fgfr2* resulted in a partial reversion of the phenotype. There was no apparent rescue of the phenotype seen in the growth plate and the primary ossification center as *Fgfr1* and *Fgfr3* are the

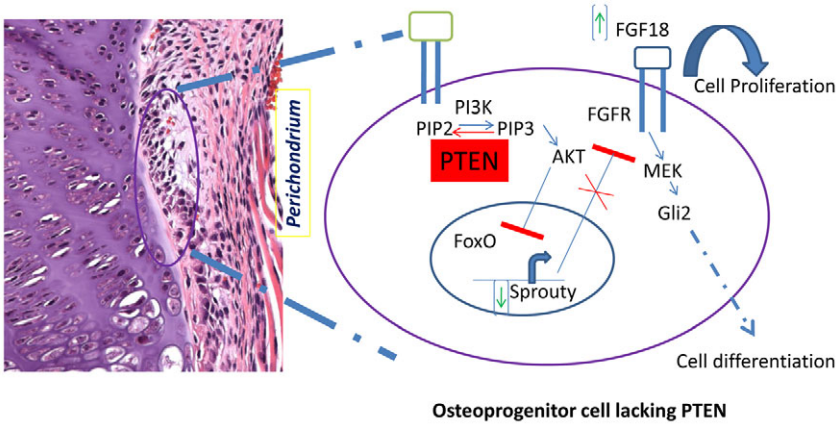

Fig. 10. Model of the mechanism through which PTEN regulates osteoprogenitors. Osteoblast progenitors in the perichondrium of the long bone are targeted by using *Dermo1*cre. When *Pten* is deleted in these cells, PI3K signaling effector AKT is activated. This leads to inactivation of FOXO transcriptional factors by sequestering them in the cytoplasm. This leads to downregulation of *Spry2* (also known as sprouty2), a negative regulator of FGF signaling. In the *Pten* conditional knockout (cko), we also observe an increase in FGF18, which leads to an increase in FGF-dependent MAP Kinase activation and cell proliferation. The increase in MAP Kinase in turn activates MEK and ERK, which activate the transcription factor GLI2, leading to increased osteoblast cell differentiation.

major receptors expressed in the growth plate whereas osteoblasts express all three receptors, suggesting that the loss of one allele of *Fgfr2* is not enough to rescue the *Pten* cko phenotype completely. Even then, these data provide strong evidence that increased FGF signaling contributes to the phenotype of increased bone following disruption of *Pten* in osteoprogenitor cells.

Increased FGF signaling in the *Pten* cko and its effect on hedgehog signaling

We showed increased expression of FGF18 combined with reduced SPRY2, which implies increased FGFR signaling. Additional evidence of increased FGF signaling followed from studies of mitogen-activated protein kinase (MAP kinase) activity. Activated MAP kinases are a hallmark of receptor tyrosine signaling. Therefore, we examined whether deletion of PTEN increased activation of the MAP kinases ERK1 (MAPK3 – Mouse Genome Informatics) and ERK2 (MAPK1 – Mouse Genome Informatics). Using cultured osteoblasts lacking PTEN we found an increase in the phosphorylation of ERK1 and ERK2. This coincided with increased nuclear localization of ERK. This discovery is germane both to the proliferation and differentiation of osteoprogenitor cells. Activation of ERK is a well-recognized signal for the stimulation of activation of cell proliferation (Pagès et al., 1993; Seger and Krebs, 1995). Thus, osteoprogenitor cell expansion in the absence of PTEN is likely to require increased MAP kinase signaling. The effects on osteoprogenitor cell differentiation are likely to be coupled to the increase in GLI2. Studies show that GLI2 is stabilized in the presence of activated MAP kinases, possibly due to direct phosphorylation of the transcription factor (Riobó et al., 2006). Our unpublished data demonstrates that active MAPK signaling stabilizes GLI2 protein by increasing its half life (Z. Liu and M.C.N. unpublished). Further evidence for stabilization of GLI2 has been shown previously by Brewester et al. (Brewester et al., 2000) who showed that GLI2 regulation is cycloheximide dependent. Therefore, the activation of differentiation might rely on activation and/or stabilization of the transcription factor GLI2.

Cell autonomous osteoblast differentiation

Our data demonstrate increased growth and differentiation of osteoprogenitor cells following conditional deletion of *Pten* in mice. These data suggested that these were direct, cell-autonomous effects. To test this possibility, we examined the differentiation of osteoprogenitor cells derived from the calvarium of newborn mice. *Pten*-null osteoprogenitor cells were prepared from the calvarium of mice with floxed *Pten* alleles. Subsequently, the cells were infected with adenoviruses transducing cre-recombinase or GFP. Similarly, cells were prepared from the calvarium of cko mice. Using real-time PCR we showed an increase in osterix, osteocalcin and *Fgf18* in the *Pten*-deleted calvarial osteoblasts. Similar results were found in primary osteoblasts isolated from *Pten* ckos (see Fig. S3 in the supplementary material). These data strongly support a cell-autonomous pathway of osteoblast differentiation in the perichondrium of *Pten* cko mice.

Additional evidence of cell-autonomous differentiation was derived from organ culture experiments. We prepared metatarsal rudiments from 15.5 dpc mouse embryos (wild type and cko) and cultured the samples in serum-free medium. In this assay, perichondrial osteoblast development is strictly linked to chondrocyte hypertrophy. We reasoned that if amplified osteoblastogenesis is secondary to accelerated or magnified chondrocyte maturation in *Pten* ckos, then this will be recapitulated in the organ culture assay. We observed, however, no increase in bone formation in the *Pten* cko metatarsals relative to the wild-type controls. Moreover, the onset of hypertrophy was similar in wild-type and cko rudiments. This leads us to conclude that the dramatic increase in perichondrial bone formation is not due to augmented chondrocyte hypertrophy in the ckos. In view of the results discussed, we propose the following model which discusses the mechanism through which bone formation is regulated in the absence of Pten (Fig. 10). Osteoprogenitor cells in the perichondrium lacking *Pten* regulate osteoblast proliferation and differentiation by activating FGF signaling. Activation of FGF signaling due to increased ligand (FGF18) and decreased SPRY2 leads to stabilization of GLI2 protein levels, which in turn promotes osteoblast differentiation. These data also show that FOXO3 has a role in regulating FGF signaling. The importance of the FOXO group of transcriptional factors in bone development has been shown recently. Ambrogini et al. (Ambrogini et al., 2010) showed that FOXOs regulate osteoblasts via oxidative stress pathways and Rached et al. (Rached et al., 2010) demonstrated regulation of osteocalcin gene expression by FOXO1. We provide additional evidence that FOXOs regulate bone development through antagonism of *Fgf18* expression.

Acknowledgements

This study was submitted as part of a PhD thesis to the Department of Biochemistry, UTHSCSA by A.R.G. We thank Dr Charles Keller and Suresh Prajapati (GCCRI, San Antonio) for help with microCT analysis. This study was funded by NIH grant R01AR053100 to MCN. Deposited in PMC for release after 12 months.

Competing interests statement
The authors declare no competing financial interests.

Supplementary material
Supplementary material for this article is available at
http://dev.biologists.org/lookup/suppl/doi:10.1242/dev.058016/-/DC1

References

Ambrogini, E., Maria, A., Marta, M.-M., Ji-Hye, P., Ronald, A. D., Li, H., Goellner, J., Weinstein, R. S., Jilka, R. L., O'Brien, C. A. et al. (2010). FoxO-mediated defense against oxidative stress in osteoblasts is indispensable for skeletal homeostasis in mice. *Cell Metab.* **11**, 136-146.

Brewster, R., Mullor, J. L. and Ruiz i Altaba, A. (2000). Gli2 functions in FGF signaling during antero-posterior patterning. *Development* **127**, 4395-4405.

Brunet, A., Bonni, A., Zigmond, M. J., Lin, M. Z., Juo, P., Hu, L. S., Anderson, M. J., Arden, K. C., Blenis, J. and Greenberg, M. E. (1999). Akt promotes cell survival by phosphorylating and inhibiting a Forkhead transcription factor. *Cell* **96**, 857-868.

Colnot, C., Lu, C., Hu, D. and Helms, J. A. (2004). Distinguishing the contributions of the perichondrium, cartilage, and vascular endothelium to skeletal development. *Dev. Biol.* **269**, 55-69.

Cooper, M. K., Wassif, C. A., Krakowiak, P. A., Taipale, J., Gong, R., Kelley, R. I., Porter, F. D. and Beachy, P. A. (2003). A defective response to Hedgehog signaling in disorders of cholesterol biosynthesis. *Nat. Genet.* **33**, 508-513.

Ford-Hutchinson, A. F., Ali, Z., Lines, S. E., Hallgrímsson, B., Boyd, S. K. and Jirik, F. R. (2007). Inactivation of Pten in osteo-chondroprogenitor cells leads to epiphyseal growth plate abnormalities and skeletal overgrowth. *J. Bone Miner. Res.* **22**, 1245-1259.

Geng, H., Lan, R., Wang, G., Siddiqi, A. R., Naski, M. C., Brooks, A. I., Barnes, J. L., Saikumar, P., Weinberg, J. M. and Venkatachalam, M. A. (2009). Inhibition of autoregulated TGFbeta signaling simultaneously enhances proliferation and differentiation of kidney epithelium and promotes repair following renal ischemia. *Am. J. Pathol.* **174**, 1291-1308.

Gross, I., Bassit, B., Benezra, M. and Licht, J. D. (2001). Mammalian sprouty proteins inhibit cell growth and differentiation by preventing ras activation. *J. Biol. Chem.* **276**, 46460-46468.

Hacohen, N., Kramer, S., Sutherland, D., Hiromi, Y. and Krasnow, M. A. (1998). *sprouty* encodes a novel antagonist of FGF signaling that patterns apical branching of the Drosophila airways. *Cell* **92**, 253-263.

Hsieh, S.-C., Chen, N.-T. and Lo, S. H. (2009). Conditional loss of PTEN leads to skeletal abnormalities and lipoma formation. *Mol. Carcinog.* **48**, 545-552.

Kapadia, R. M., Guntur, A. R., Reinhold, M. I. and Naski, M. C. (2005). Glycogen synthase kinase 3 controls endochondral bone development: contribution of fibroblast growth factor 18. *Dev. Biol.* **285**, 496-507.

Karsenty, G. (1999). The genetic transformation of bone biology. *Genes Dev.* **13**, 3037-3051.

Kronenberg, H. (2003). Developmental regulation of the growth plate. *Nature* **423**, 332.

Li, J., Yen, C., Liaw, D., Podsypanina, K., Bose, S., Wang, S. I., Puc, J., Miliaresis, C., Rodgers, L., McCombie, R. et al. (1997). PTEN, a putative protein tyrosine phosphatase gene mutated in human brain, breast, and prostate cancer. *Science* **275**, 1943-1947.

Li, L., Cserjesi, P. and Olson, E. N. (1995). Dermo-1: a novel twist-related bHLH protein expressed in the developing dermis. *Dev. Biol.* **172**, 280-292.

Liu, X., Bruxvoort, K. J., Zylstra, C. R., Liu, J., Cichowski, R., Faugere, M.-C., Bouxsein, M. L., Wan, C., Williams, B. O. and Clemens, T. L. (2007). Lifelong accumulation of bone in mice lacking Pten in osteoblasts. *Proc. Natl. Acad. Sci. USA* **104**, 2259-2264.

Liu, Z., Xu, J., Colvin, J. S. and Ornitz, D. M. (2002). Coordination of chondrogenesis and osteogenesis by fibroblast growth factor 18. *Genes Dev.* **16**, 859.

Livak, K. J. and Schmittgen, T. D. (2001). Analysis of relative gene expression data using real-time quantitative PCR and the 2-[delta][delta]CT method. *Methods* **25**, 402-408.

McLeod, M. J. (1980). Differential staining of cartilage and bone in whole mouse fetuses by alcian blue and alizarin red S. *Teratology* **22**, 299-301.

Miraoui, H. and Marie, P. J. (2010). Fibroblast growth factor receptor signaling crosstalk in skeletogenesis. *Sci. Signal.* **3**, re9.

Muenke, M., Schell, U., Hehr, A., Robin, N. H., Losken, H. W., Schinzel, A., Pulleyn, L. J., Rutland, P., Reardon, W. and Malcolm, S. (1994). A common mutation in the fibroblast growth factor receptor 1 gene in Pfeiffer syndrome. *Nat. Genet.* **8**, 269-274.

Myers, M. P., Pass, I., Battyl, H., Van der Kaay, J., Stolarov, J. P., Hemmings, B. A., Wigler, M. H., Downes, C. P. and Tonks, N. K. (1998). The lipid phosphatase activity of PTEN is critical for its tumor supressor function. *Proc. Natl. Acad. Sci. USA* **95**, 13513-13518.

Naski, M. C., Wang, Q., Xu, J. and Ornitz, D. M. (1996). Graded activation of fibroblast growth factor receptor 3 by mutations causing achondroplasia and thanatophoric dysplasia. *Nat. Genet.* **13**, 233-237.

Naski, M. C., Colvin, J. S., Coffin, J. D. and Ornitz, D. M. (1998). Repression of hedgehog signaling and BMP4 expression in growth plate cartilage by fibroblast growth factor receptor 3. *Development* **125**, 4977-4988.

Ohbayashi, N., Shibayama, M., Kurotaki, Y., Imanishi, M., Fujimori, T., Itoh, N. and Takada, S. (2002). FGF18 is required for normal cell proliferation and differentiation during osteogenesis and chondrogenesis. *Genes Dev.* **16**, 870-879.

Ornitz, D. M. (2005). FGF signaling in the developing endochondral skeleton. *Cytokine Growth Factor Rev.* **16**, 205-213.

Pagès, G., Lenormand, P., Allemain, G., Chambard, J. C., Meloche. S. and Pouyssagur, J. (1993). Mitogen-activated protein kinases p42mapk and p44mapk are required for fibroblast proliferation. *Proc. Natl. Acad. Sci. USA* **90**, 8319-8323.

Paik, J.-H., Kollipara, R., Chu, G., Ji, H., Xiao, Y., Ding, Z., Miao, L., Tothova, Z., Horner, J. W., Carrasco, D. R. et al. (2007). FoxOs are lineage-restricted redundant tumor suppressors and regulate endothelial cell homeostasis. *Cell* **128**, 309-323.

Peng, X.-D., Xu, P.-Z., Chen, M.-L., Windgassen, A. H., Skeen, J., Jacobs, J., Sundararajan, D., Chen, W. S., Crawford, S. E., Coleman, K. G. et al. (2003). Dwarfism, impaired skin development, skeletal muscle atrophy, delayed bone development, and impeded adipogenesis in mice lacking Akt1 and Akt2. *Genes Dev.* **17**, 1352-1365.

Rached, M.-T., Kode, A., Silva, B. C., Jung, D. Y., Gray, S., Ong, H., Paik, J.-H., DePinho, R. A., Kim, J. K., Karsenty, G. et al. (2010). FoxO1 expression in osteoblasts regulates glucose homeostasis through regulation of osteocalcin in mice. *J. Clin. Invest.* **120**, 357-368.

Reardon, W., Winter, R. M., Rutland, P., Pulleyn, L. J., Jones, B. M. and Malcolm, S. (1994). Mutations in the fibroblast growth factor receptor 2 gene cause Crouzon syndrome. *Nat. Genet.* **8**, 98.

Reinhold, M. I. and Naski, M. C. (2007). Direct interactions of Runx2 and canonical Wnt signaling induce FGF18. *J. Biol. Chem.* **282**, 3653-3663.

Reinhold, M. I., Kapadia, R. M., Liao, Z. and Naski, M. C. (2006). The Wnt-inducible transcription factor Twist1 inhibits chondrogenesis. *J. Biol. Chem.* **281**, 1381-1388.

Riobó, N. A., Lu, K., Ai, X., Haines, G. M. and Emerson, C. P., Jr. (2006). Phosphoinositide 3-kinase and Akt are essential for Sonic Hedgehog signaling. *Proc. Natl. Acad. Sci. USA* **103**, 4505-4510.

Rousseau, F., Bonaventure, J., Legeai-Mallet, L., Pelet, A., Rozet, J. M., Maroteaux, P., Le Merrer, M. and Munnich, A. (1994). Mutations in the gene encoding fibroblast growth factor receptor-3 in achondroplasia. *Nature* **371**, 252.

Seger, R. and Kerbs, E. G. (1995). The MAPK signaling cascade. *FASEB J.* **9**, 726-735.

Stambolic, V., Suzuki, A., de la Pompa, J. L., Brothers, G. M., Mirtsos, C., Sasaki, T., Ruland, J., Penninger, J. M., Siderovski, D. P. and Mak, T. W. (1998). Negative regulation of PKB/Akt-dependent cell survival by the tumor suppressor PTEN. *Cell* **95**, 29-39.

Sun, H., Lesche, R., Li, D. M., Liliental, J., Zhang, H., Gao, J., Gavrilova, N., Mueller, B., Liu, X. and Wu, H. (1999). PTEN modulates cell cycle progression and cell survival by regulating phosphatidylinositol 3,4,5,-trisphosphate and Akt/protein kinase B signaling pathway. *Proc. Natl. Acad. Sci. USA* **96**, 6199-6204.

Suzuki, A., Yamaguchi, M. T., Ohteki, T., Sasaki, T., Kaisho, T., Kimura, Y., Yoshida, R., Wakeham, A., Higuchi, T., Fukumoto, M. et al. (2001). T cell-specific loss of Pten leads to defects in central and peripheral tolerance. *Immunity* **14**, 523-534.

Vasquez, S. X., Hansen, M. S., Bahadur, A. N., Hockin, M. F., Kindlmann, G. L., Nevell, L., Wu, I. Q., Grunwald, D. J., Weinstein, D. M., Jones, G. M. et al. (2008). Optimization of volumetric computed tomography for skeletal analysis of model genetic organisms. *Anat. Rec.* **291**, 475-487.

Vortkamp, A., Lee, K., Lanske, B., Segre, G. V., Kronenberg, H. M. and Tabin, C. J. (1996). Regulation of rate of cartilage differentiation by indian hedgehog and PTH-related protein. *Science* **273**, 613-622.

Yang, G., Sun, Q., Teng, Y., Li, F., Weng, T. and Yang, X. (2008). PTEN deficiency causes dyschondroplasia in mice by enhanced hypoxia-inducible factor 1α signaling and endoplasmic reticulum stress. *Development* **135**, 3587-3597.

Yeh, L. C., Adamo, M. L., Kitten, A. M., Olson, M. S. and Lee, J. C. (1996). Osteogenic protein-1-mediated insulin-like growth factor gene expression in primary cultures of rat osteoblastic cells. *Endocrinology* **137**, 1921.

Yu, K., Xu, J., Liu, Z., Sosic, D., Shao, J., Olson, E. N., Towler, D. A. and Ornitz, D. M. (2003). Conditional inactivation of FGF receptor 2 reveals an essential role for FGF signaling in the regulation of osteoblast function and bone growth. *Development* **130**, 3063-3074.

Zhao, M., Harris, S. E., Horn, D., Geng, Z., Nishimura, R., Mundy, G. R. and Chen, D. (2002). Bone morphogenetic protein receptor signaling is necessary for normal murine postnatal bone formation. *J. Cell Biol.* **157**, 1049-1060.